AD-A105 970 NAVAL SURFACE WEAPONS CENTER SILVER SPRING MD F/G 20/4
CORRELATION OF INSTANTANEOUS IMPACT DRAG COEFFICIENTS FOR VERTI--ETC(U)
JUN 80 C W SMITH
UNCLASSIFIED NSWC/TR-80-243 NL

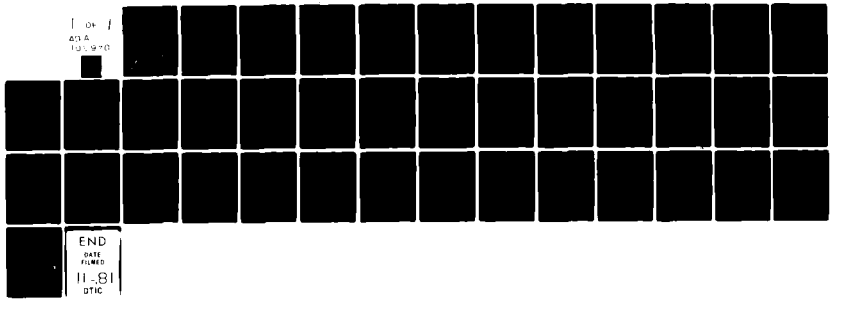

END
DATE FILMED
11-81
DTIC

LEVEL

NSWC TR 80-243

AD A105970

CORRELATION OF INSTANTANEOUS IMPACT DRAG COEFFICIENTS FOR VERTICAL WATER ENTRY

BY CHARLES W. SMITH

UNDERWATER SYSTEMS DEPARTMENT

JUNE 1980

Approved for public release, distribution unlimited.

NAVAL SURFACE WEAPONS CENTER

Dahlgren, Virginia 22448 • Silver Spring, Maryland 20910

81 10 21

UNCLASSIFIED
SECURITY CLASSIFICATION OF THIS PAGE (When Data Entered)

REPORT DOCUMENTATION PAGE	READ INSTRUCTIONS BEFORE COMPLETING FORM
1. REPORT NUMBER (14) NSWC/TR-80-243	2. GOVT ACCESSION NO. AD-A095 963	3. RECIPIENT'S CATALOG NUMBER
4. TITLE (and Subtitle) (6) CORRELATION OF INSTANTANEOUS IMPACT DRAG COEFFICIENTS FOR VERTICAL WATER ENTRY.		5. TYPE OF REPORT & PERIOD COVERED (9) Interim Technical rept. Oct 1979 - Sep 1980
		6. PERFORMING ORG. REPORT NUMBER
7. AUTHOR(s) Mr. C. Smith (10) Charles W. Smith		8. CONTRACT OR GRANT NUMBER(s) 61153N (16) SR023 04
9. PERFORMING ORGANIZATION NAME AND ADDRESS Naval Surface Weapon Center White Oak Silver Spring, Md. 20910 (17)		10. PROGRAM ELEMENT, PROJECT, TASK AREA & WORK UNIT NUMBERS 61153N, SR02301 SR023101, U54AA
11. CONTROLLING OFFICE NAME AND ADDRESS (11)		12. REPORT DATE June 1980
		13. NUMBER OF PAGES (12) 40
14. MONITORING AGENCY NAME & ADDRESS (if different from Controlling Office)		15. SECURITY CLASS. (of this report) UNCLASSIFIED
		15a. DECLASSIFICATION/ DOWNGRADING SCHEDULE

16. DISTRIBUTION STATEMENT (of this Report)

Approved for public release; Distribution unlimited

17. DISTRIBUTION STATEMENT (of the abstract entered in Block 20, if different from Report)

18. SUPPLEMENTARY NOTES

19. KEY WORDS (Continue on reverse side if necessary and identify by block number)

Water entry	sphere	Correlation
vertical	ogives	
drag	cusps	
cones	hemisphere	

20. ABSTRACT (Continue on reverse side if necessary and identify by block number)

(U) A theoretical model for predicting the height of the heaved water surface about a cone during vertical water entry was developed. The successful comparison of the predictions of the theoretical model with experimental data encouraged an extension of the model to include a method for predicting the impact drag force during vertical water entry. Experimental data for cones, ogives, cusps and sphere were successfully correlated indicating the usefulness of the model for correlating impact drag forces for a wide range of configurations.

DD FORM 1473 EDITION OF 1 NOV 65 IS OBSOLETE

UNCLASSIFIED 443563
SECURITY CLASSIFICATION OF THIS PAGE (When Data Entered)

FOREWORD

This report is a result of the continuing effort of the Naval Surface Weapons Center in the understanding of water-entry phenomena. The research reported herein was supported entirely by NAVSEA Code 63R31 under task SR0230100. The author would like to acknowledge Dr. Thomas Pierce of NAVSEA for his advice and interest in this program.

F. B. SANCHEZ
By direction

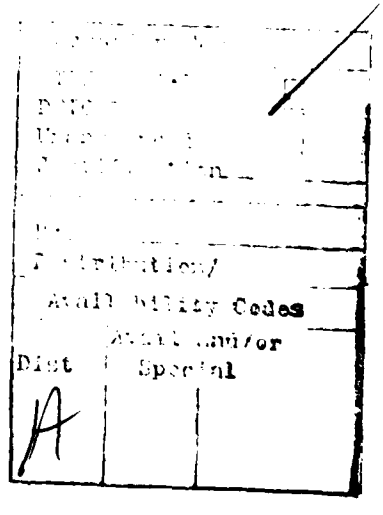

CONTENTS

ILLUSTRATIONS

TABLES

LIST OF SYMBOLS

A	DEPTH OF PENETRATION OF ELLIPSOIDAL MODEL
A_1, A_2, A_3,	EMPIRICAL CONSTANTS FOR IMPACT DRAG COEFFICIENT
a	HALF-LENGTH OF THE AXISYMMETRIC ELLIPSOIDAL MODEL
b	MAXIMUM RADIUS OF THE AXISYMMETRIC ELLIPSOID, RADIUS OF WATER-ENTRY BODY AT WETTED PERIMETER WITH THE HEAVED FREE SURFACE
C_d	INSTANTANEOUS IMPACT DRAG COEFFICIENT
$C_{d_{max}}$	MAXIMUM VALUE OF INSTANTANEOUS IMPACT DRAG COEFFICIENT
C_p	PRISMATIC COEFFICIENT OF WATER-ENTRY BODY, VOLUME/π b^2 h
F	INSTANTANEOUS DRAG FORCE
H	DEPTH OF PENETRATION OF THE WATER-ENTRY BODY
h	HEIGHT OF THE WETTED PERIMETER (WITH THE HEAVED FREE SURFACE) AS MEASURED FROM THE SUBMERGED TIP OF THE WATER-ENTRY BODY
K_1	INERTIAL FACTOR FOR AXIAL MOTION OF ELLIPSOIDS
M	'ADDED MASS' OF THE WATER-ENTRY BODY
P	AXIAL MOMENTUM OF THE FLUID
r	RADIAL COORDINATE (CYLINDRICAL)
r_o	MAXIMUM OR REFERENCE RADIUS OF WATER-ENTRY BODY
t	TIME
U	AXIAL VELOCITY (CYLINDRICAL COORDINATES)
w	WETTING FACTOR
X	AXIAL COORDINATE (CYLINDRICAL), ORIGIN IN THE PLANE OF THE HEAVED FREE SURFACE

LIST OF SYMBOLS (Cont'd)

z	AXIAL COORDINATE (CYLINDRICAL), ORIGIN IN THE PLANE OF THE ORIGINAL UNDISTURBED FREE SURFACE
α	CONE ANGLE OF WATER-ENTRY BODY
α_o	ELLIPSOIDAL CONSTANT
β	ANGLE SUBTENDED BY THE ARC OF CURVATURE OF THE WATER-ENTRY BODY (NEGATIVE VALUE FOR CUSPS)
Γ	MOMENTUM CORRECTION TERM
γ	FINENESS RATIO OF ELLIPSOIDAL MODEL
Δ	DENOTES CHANGE IN VALUE OF
η	HEIGHT OF THE HEAVED FREE SURFACE
λ	EQUIVALENT INERTIAL FACTOR FOR AXIAL MOTION OF WATER-ENTRY BODY
ρ	MASS DENSITY OF WATER

SUPERSCRIPTS

$\dot{}$	DENOTES DIFFERENTIATION WITH RESPECT To t
$'$	DENOTES DIFFERENTIATION WITH RESPECT To h
$\bar{}$	DENOTES AVERAGE VALUE OF TEST DATA

INTRODUCTION

The development of naval weapons requiring delivery through an air-water interface necessitates an understanding of the various water-entry phenomena which have a predominant influence on the trajectory of a water-entry vehicle from initial impact until the attrition of the water-entry cavity. To address this need the large Hydroballistics Facility and Associated Pilot Tank were constructed at the Naval Surface Weapons Center/White Oak Laboratory specifically for the study of water-entry phenomena. A program was initiated in 1967 to obtain basic vertical water-impact acceleration data for conical shapes. This effort was later extended to include ogives, cusps and the sphere. A digital program, Reference 1, has recently been written to predict the forces during water-entry. This code requires the use of approximate procedures for estimating the wetting factor (height of the heaved water surface wetting the cone) and for estimating the shape of the cavity.

A concurrent program was also initiated in 1967 to study the behavior of the water-entry cavity. In a recent study, Reference 2, an analytical model was developed to predict the dynamic behavior and shape of the water-entry cavity, neglecting the effect of the free surface. This model successfully predicts the frequency response of the cavity which occurs after cavity closure. The model was developed from energy considerations and assumed that the fluid velocity was in a direction normal to the velocity of the water-entry vehicle. Near the free surface this is obviously not true. The compliance of the free surface results in a large vertical velocity component as evinced by the heaving of the free surface and the splash that occurs in the neighborhood surrounding the point of water impact. In extending the study to include the effect of the free surface, a theoretical model for predicting the heaving motion of the free surface was developed. This model successfully predicts the wetting factors for cones obtained experimentally as reported in Reference 3. The use of this model in the digital program of Reference 1 should eliminate the need for the approximate methods presently employed.

---

[1]Wardlaw, A. B., Morrison, A. M. and Baldwin, J. L., "Prediction Of Impact Pressures, Forces, and Moments During Vertical And Oblique Water-Entry", NSWC/WOL/TR 77-16, January 1977.

[2]Smith, C. W., "Experimental Investigation of the Behavior of Vertical Water-Entry Cavities", NSWC/WOL/TR 78-135, September 1978.

[3]Baldwin, J. L., "Vertical Water-Entry of Cones" NOLTR 71-25, February 1971.

The ability of the model to predict the wetting factors for cones encouraged an extension of the model to include a method for predicting the impact drag force during vertical water-entry. Successful correlation of the cone data reported in Reference 3 was obtained after incorporating a momentum correction to the theoretical model. Only two empirical constants were necessary to correlate the cone data reported in Reference 3 (10, 15, 20, 30, 45, 60, 90, 120 and 140 degree cones). The model was then extended to incorporate a changing prismatic coefficient (for displaced volume). Experimental data for the sphere, Reference 4, and for ogives and cusps, Reference 5, were then correlated. For the sphere and each ogive and cusp, a different set of empirical constants was required. The author's hope that one set of empirical constants might correlate all geometries was not realized. Correlation of the empirical constants appears to be a possibility, however, test data for additional geometries must be obtained and correlated before this can reasonably be attempted.

---

[3] See footnote 3 on page 5

[4] Baldwin, J. L. and Steves, H. K., "Vertical Water-Entry of Spheres", NSWC/WOL/TR 75-49, May 1975.

[5] Baldwin, J. L., "Vertical Water-Entry of Some Ogives, Cones, and Cusps", NSWC/WOL/TR 75-20, March 1975.

THEORETICAL MODEL FOR THE HEAVED FREE SURFACE

Shiffman and Spencer, in Reference 6, employed an approximating ellipsoid to obtain an expression for the wetting factor and drag coefficient for the vertical water-entry of cones. Their model assumed that the approximating ellipsoid should have a fineness ratio, γ, such that:

$$\gamma = \frac{a}{b} = \cot\left(\frac{\alpha}{2}\right) \tag{1}$$

This assumption implies that the velocity of the approximating ellipsoid is equal to the velocity of penetration of the cone. In modifying Shiffman and Spencer's analysis to obtain better agreement with the experimental data for cones in Reference 3, no assumption was made for the fineness ratio of the ellipsoid. Figure 1 defines the nomenclature used to describe the geometry of the cone and ellipsoid. In this figure, the depth of penetration of the ellipsoid is defined:

$$A \equiv a - (h-H) \tag{2}$$

and the velocity of penetration is obtained by differentiating equation (2):

$$\dot{A} \equiv \dot{a} - (\dot{h}-\dot{H}) \tag{3}$$

To account for the compliance of the free surface it was assumed, as did Shiffman and Spencer, that the heaved free surface:

$$\eta\,(r,\,t) = -\,z \tag{4}$$

is located in the equatorial plane of the ellipsoid ($x = o$). In this plane the velocity of the fluid, and therefore the free surface, is vertically upward. On the intersection of the heaved free surface with the ellipsoid, the fluid velocity, from equation (A-29) of Appendix A, is:

$$\dot{h} - \dot{H} = \dot{\eta}\,\Big|_{r=b} = K_1\,\dot{A} \tag{5}$$

where K_1 is defined in Appendix A, equation (A-20).

A third equation is obtained by performing a mass balance:

$$2\pi\rho \int_b^\infty \dot{\eta} r\,dr + \rho\pi b^2\,(\dot{h}-\dot{H}) = \rho\pi b^2\,C_p\,\dot{h} \tag{6}$$

where it is assumed that the correlation factor, C_p, is the prismatic coefficient of the entering body.

---

[6] Shiffman, M. and Spencer, D. C., "Force of Impace On a Cone Striking a Water Surface (Vertical Entry)", Comm. Pure and Appl. Math., Vol IV (1951).

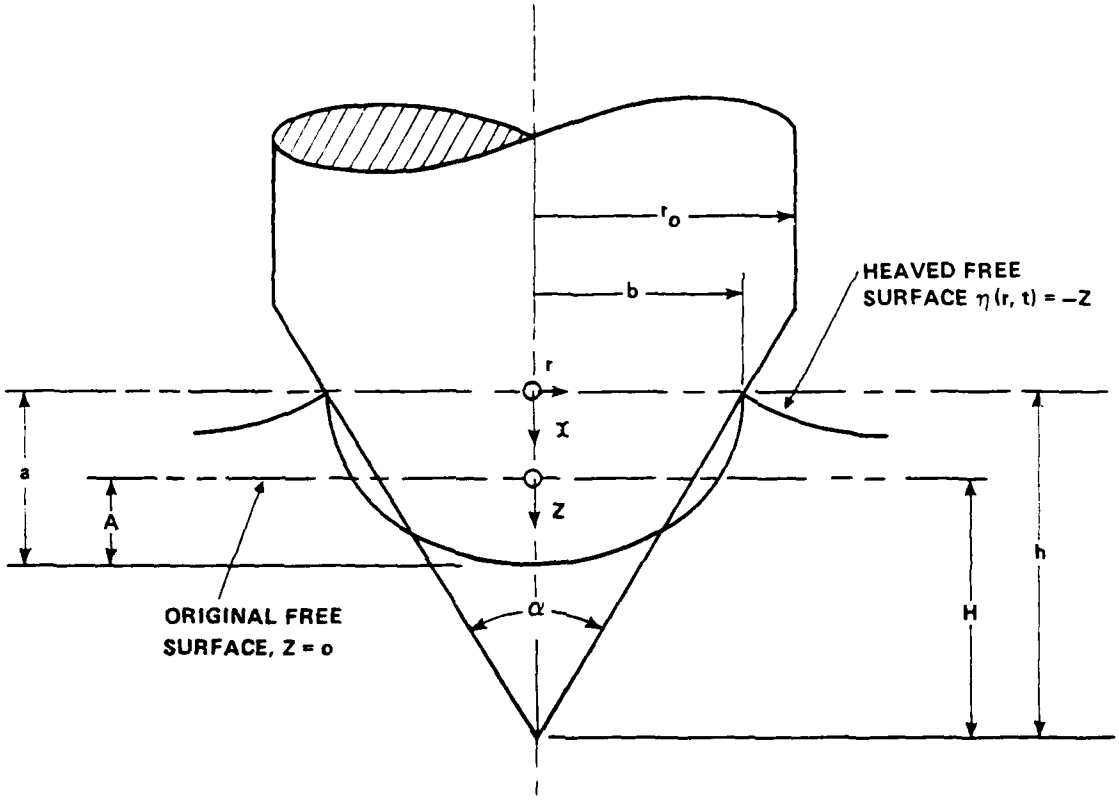

FIGURE 1 ELLIPSOID FOR WATER ENTRY MODEL

Equation (6) can be written, after substituting equation (A-35) from Appendix A for the first term:

$$\dot{A} + (\dot{h}-\dot{H}) = C_p\dot{h} \tag{7}$$

Since, for an arbitrary configuration, b and C_p can be written as functions of h, it is more convenient to use h as the independent variable. Equations (3), (5) and (7) then become, respectively:

$$A' \equiv a' - (1 - H') \tag{8}$$

$$1 - H' = K_1 A' \tag{9}$$

$$A' + (1 - H') = C_p \tag{10}$$

To obtain an expression for a and γ, A' from equation (8) is substituted into equation (10):

$$a' = C_p \tag{11}$$

integrating:

$$a = \int_o^h C_p \, dh \tag{12}$$

and dividing by b:

$$\gamma = \frac{a}{b} = \frac{1}{b} \int_o^h C_p \, dh \tag{13}$$

To obtain an expression for h-H and the wetting factor, equation (9) is integrated:

$$h - H = \int_o^h K_1 A' \, dh \tag{14}$$

Substituting equation (9) for $(1 - H^1)$ into equation (10):

$$(1 + K_1) A' = C_p$$

$$K_1 A' = \frac{K_1}{1 + K_1} C_p = \frac{\alpha_o}{2} C_p \tag{15}$$

where α_o is defined in Appendix A, equation (A-22), as a function of the fineness ratio, γ. Equation (14) can now be written:

$$h - H = \int_o^h \frac{\alpha_o}{2} C_p \, dh \tag{16}$$

and the wetting factor:

$$w \equiv \frac{h}{H} = \frac{1}{1 - \frac{1}{h} \int_o^h \frac{\alpha_o}{2} C_p dh} \tag{17}$$

For a cone, $C_p = 1/3$, $b = h \tan (\frac{\alpha}{2})$ and equation (13) becomes:

$$\gamma = \frac{1}{3} \frac{h}{b} = \frac{1}{3} \cot (\frac{\alpha}{2}) \tag{18}$$

For a given cone angle α, γ and α_o are constants and equation (17) becomes:

$$w = \frac{1}{1 - \alpha_o/6} \tag{19}$$

The calculated wetting factors, using equation (19), are tabulated in Table 1 and compared with the experimental data from Reference 3. The predictions are in good agreement with the experimental results and well within the variation of experimental results.

MODEL FOR THE IMPACT DRAG FORCE

To obtain the impact drag force, the principle of conservation of momentum is employed. Due to rotational symmetry, the total momentum of the fluid is directed vertically downward. From equation (A-40) of Appendix A:

$$P = M\dot{H} = 2\pi\rho \iint U r dr dx = \frac{2}{3} \rho\pi b^2 \, a \, K_1 \, \dot{A} \tag{20}$$

An expression for the 'added mass' is obtained from equation (20):

$$M = \frac{2}{3} \rho\pi b^2 \, a\lambda \tag{21}$$

where:

$$\lambda \equiv K_1 \frac{\dot{A}}{\dot{H}} = \frac{K_1 A'}{H} \tag{22}$$

The force on the body entering the water is directed vertically upward and is equal to:

$$F = \dot{P} = \dot{M}\dot{H} = \frac{M'}{H'} \dot{H}^2 \tag{23}$$

[3] See footnote 3 on page 5

TABLE 1

WETTING FACTORS FOR CONES, $w = h/H$

Cone Angle, α Degrees	Experimental Results, Ref. 3			Predicted Values	
	Average	Variation, %		Eq.(19)	$(w-\bar{w})/\bar{w}$
	$\bar{w}$	Lowest (-)	Highest (+)	w	%
10	-			1.0275	-
15	-			1.0465	-
20	1.0609	10.39	10.34	1.0655	+ .43
30	1.1038	10.33	11.42	1.1018	- .18
45	1.1290	11.25	7.71	1.1507	+1.92
60	1.1661	8.65	11.73	1.1937	+2.37
90	1.2406	8.19	13.11	1.2687	+2.27
120	1.3101	11.45	11.42	1.3381	+2.14
140	1.3977	4.34	13.35	1.3858	- .85

where it is assumed that the velocity, $\dot{H}$, is a constant. The instantaneous impact drag coefficient is defined:

$$C_d \equiv \frac{2F}{\rho\pi r_o^2 \dot{H}^2} = \frac{2M'}{\rho\pi r_o^2 H'} = \frac{4}{3}\frac{(b^2 a\lambda)'}{r_o^2 H'} \tag{24}$$

For a cone, λ and γ are constants, $b = h \tan(\frac{\alpha}{2})$, and equation (24) can be written:

$$C_d = \frac{4}{3}\frac{\lambda}{H'}\left(\frac{b}{r_o}\right)^2 \tag{25}$$

The maximum impact force occurs when $b = r_o$:

$$C_{d_{max}} = \frac{4}{3}\frac{\lambda}{H'} \tag{26}$$

The maximum impact drag coefficients reported in Reference 3 for cones could not be adequately correlated with the use of equation (26). To obtain a model for correlating impact drag data, a momentum term was added to equation (20). In Figure 1 the expanding geometry of the water-entry body was neglected. To accommodate the increasing radius of the water-entry body, a radial velocity field proportional to $\dot{b}$ is required. To create this local radial velocity field it was assumed that an augmented vertical velocity field proportional to:

$$U = \sqrt{(\dot{b})^2 + (\dot{h}-\dot{H})^2} \tag{27}$$

is deflected by an additional impact force. As shown in Figure 2, the change in the vertical velocity field is proportional to:

$$\Delta U = \sqrt{(\dot{b})^2 + (\dot{h}-\dot{H})^2} - (\dot{h}-\dot{H}) \tag{28}$$

and the total momentum of the fluid is now assumed to be:

$$P = A_1 M\dot{H} + A_2 M\Delta U = M\dot{H}\left[A_1 + A_2\left(\frac{\Delta U}{\dot{H}}\right)\right] \tag{29}$$

where A_1 and A_2 are empirical constants to be obtained through the correlation of experimental data. The total impact force on the water-entry body becomes:

$$F = \dot{P} = \dot{M}\dot{H}\left[A_1 + A_2\,\Gamma\right] + A_2 M\dot{H}\,\dot{\Gamma}$$

$$= \dot{H}^2\left\{M'\left[A_1 + A_2\,\Gamma\right] + A_2 M\,\Gamma'\right\}/H' \tag{30}$$

where:

$$\Gamma \equiv \left(\frac{\Delta U}{\dot{H}}\right) = \left\{\sqrt{(b')^2 + (1 - H')^2} - (1 - H')\right\}/H' \tag{31}$$

[3] *See footnote 3 on page 5.*

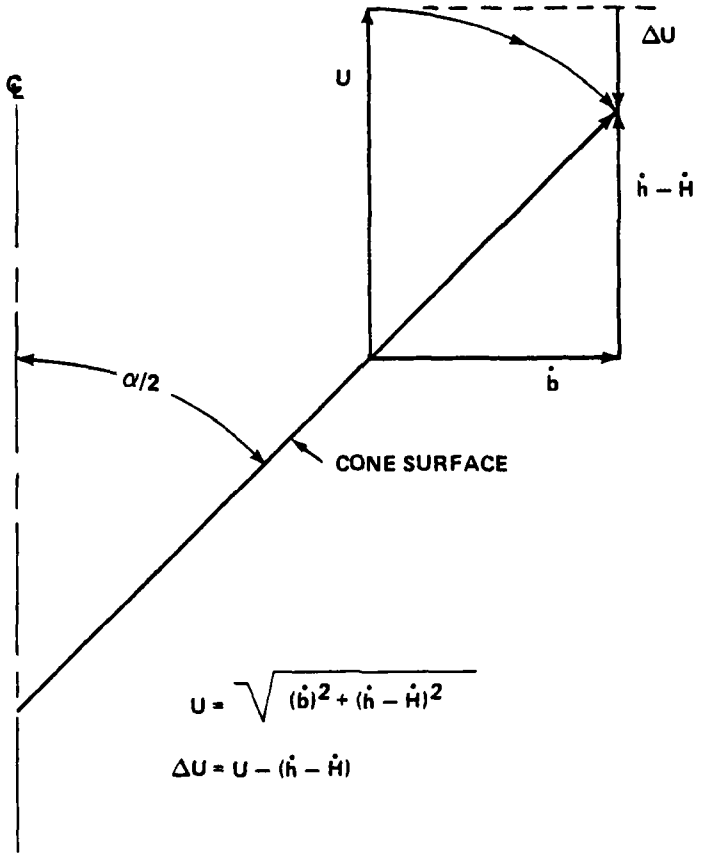

FIGURE 2 VELOCITY FIELD DEFLECTION

and the instantaneous impact drag coefficient becomes:

$$C_d \equiv \frac{2F}{\rho \pi r_o^2 \dot{H}^2}$$

$$= \frac{4}{3r_o^2 H'} \{ \left[A_1 + A_2 \Gamma \right] (b^2 a \lambda)' + A_2 (b^2 a \lambda) \Gamma' \} \tag{32}$$

An argument can be made for introducing the additional impact force in the following manner:

$$F = A_1 \ddot{M}\ddot{H} + A_2 \dot{M}\Delta U = \ddot{M}\ddot{H} \left[A_1 + A_2 \Gamma \right] \tag{33}$$

This assumes that the additional impact force is simply a surface or splash correction. If this is assumed, the last terms in equations (30) and (32) drop out. For this reason equation (32) is written in a more general manner by introducing a third empirical constant A_3, such that:

$$0 \leq A_3 \leq A_2 \tag{34}$$

equation (32) is rewritten:

$$C_d = \frac{4}{3r_o^2 H'} \{ \left[A_1 + A_2 \Gamma \right] (b^2 a \lambda)' + A_3 (b^2 a \lambda) \Gamma' \} \tag{35}$$

In summary, from equations (9) and (15):

$$H' = 1 - K_1 A' = 1 - \frac{\alpha_o}{2} C_p \tag{36}$$

from equation (22):

$$\lambda = \frac{K_1 A'}{H'} = \frac{\frac{\alpha_o}{2} C_p}{1 - \frac{\alpha_o}{2} C_p} \tag{37}$$

and a, Γ and α_o are defined by equations (12), (31) and (A-22) respectively . The radius, b, and the volume or prismatic coefficient, C_p, are obtained from geometrical considerations.

COMPARISON WITH EXPERIMENTAL DATA

The drag coefficient for the cone reduces to a simple parabolic equation:

$$C_d = \frac{4}{3} w (w - 1) \left[A_1 + A_2 \Gamma \right] \left(\frac{b}{r_o} \right)^2 \tag{38}$$

where:

$$\Gamma = \sqrt{(w \tan \frac{\alpha}{2})^2 + (w - 1)^2} - (w - 1) \tag{39}$$

$$w = \frac{1}{H^1} = \frac{1}{1 - \alpha_o/6} \tag{19}$$

$$b = h \tan \frac{\alpha}{2} \tag{40}$$

$$\gamma = \frac{1}{3} \cot \frac{\alpha}{2} \tag{18}$$

The test data in Reference 3 for the impact drag force exhibited this parabolic behavior. It was necessary, therefore, to correlate only the maximum drag coefficients:

$$C_{d_{max}} = \frac{4}{3} w (w - 1)\left[A_1 + A_2 \Gamma \right] \tag{41}$$

The results of the correlation, with $A_1 = .447$ and $A_2 = 2.1052$, are tabulated and compared with experimental data in Table 2. The correlation is in good agreement with the experimental results and is well within the variation of the test data.

Test data for the sphere, obtained from Reference 4, were correlated. Two correlations were obtained and tabulated in Table 3 for comparison with experimental results. Both correlations, the first with $A_3 = 0$, and the second with $A_3 = A_2$, are in good agreement with the test data (generally within 2.2%). The data were correlated, using least-square-fit, for penetration depths up to $H = .40\ r_o$. At this penetration depth the heaved surface on the sphere is located at $h = .658\ r_o$ where the slope on the sphere is 20 degrees. Experimental data, according to Hsu-Perry and reported in Reference 7, indicates that flow separation occurs in this neighborhood. When separation occurs, the impact drag force coefficients are no longer applicable. The drag force goes through a transition phase, from impact drag to cavity-running drag.

The method used to define the geometry of ogives and cusps is shown in Figure 3, and is given the name: α/β ogive. The hemisphere can be defined as a 90/90 ogive and the cone can be defined as a α/o ogive.

---

[3] See footnote 3 on page 5

[4] See footnote 4 on page 6

[7] May, A., "Water-Entry and the Cavity-Running Behavior of Missiles", SEA HAC/ TR 75-2, 1975.

TABLE 2

MAXIMUM IMPACT DRAG COEFFICIENTS FOR CONES, $C_{d_{max}}$

Cone Angle, α Degrees	Experimental Results, Ref. 3			Correlation, $A_1 = .4470$, $A_2 = 2.1052$	
	Average	Avariation, %		Eq. (41)	$(C_{d_{max}} - \bar{C}_{d_{max}})/\bar{C}_{d_{max}}$
	$\bar{C}_{d_{max}}$	Lowest (-)	Highest (+)	$C_{d_{max}}$	%
10	.0221	19.5	19.1	.0221	+ .4
15	.0427	9.3	9.3	.0425	- .4
20	.0696	11.1	14.5	.0677	-2.7
30	.1277	5.2	7.7	.1331	4.2
45	.2858	8.6	7.1	.2733	-4.4
60	.4608	8.5	9.4	.4766	+3.5
90	1.175	5.3	4.9	1.187	+1.0
120	2.840	7.2	9.7	2.815	- .9
140	5.547	4.8	3.9	5.483	-1.2

TABLE 3

IMPACT DRAG COEFFICIENT FOR SPHERE, Cd

Depth Of Penetration	Experimental Results Ref. 4	Correlation, Eq. (35) $A_1 = .6254$, $A_2 = .882$, $A_3 = 0$		$A_1 = 1.262$	$A_2 = A_3 = 1.083$
			$(C_d - \bar{C}_d)/\bar{C}_d$		$(C_d - \bar{C}_d)/\bar{C}_d$
H/r_o	$\bar{C}_d$	C_d	%	C_d	%
.05	.94	.975	+3.8	.954	1.5
.10	1.04	1.03	-1.0	1.03	- .8
.15	1.02	.997	-2.2	1.01	- .8
.20	.954	.933	-2.2	.948	- .6
.25	.862	.854	- .9	.864	+ .3
.30	.771	.770	- .1	.771	+ .0
.35	.683	.685	+ .3	.679	- .7
.40	.590	.602	+2.1	.596	1.0
.45	.514	.525	+2.2	.534	+3.9
.50	.457	.455	- .4		

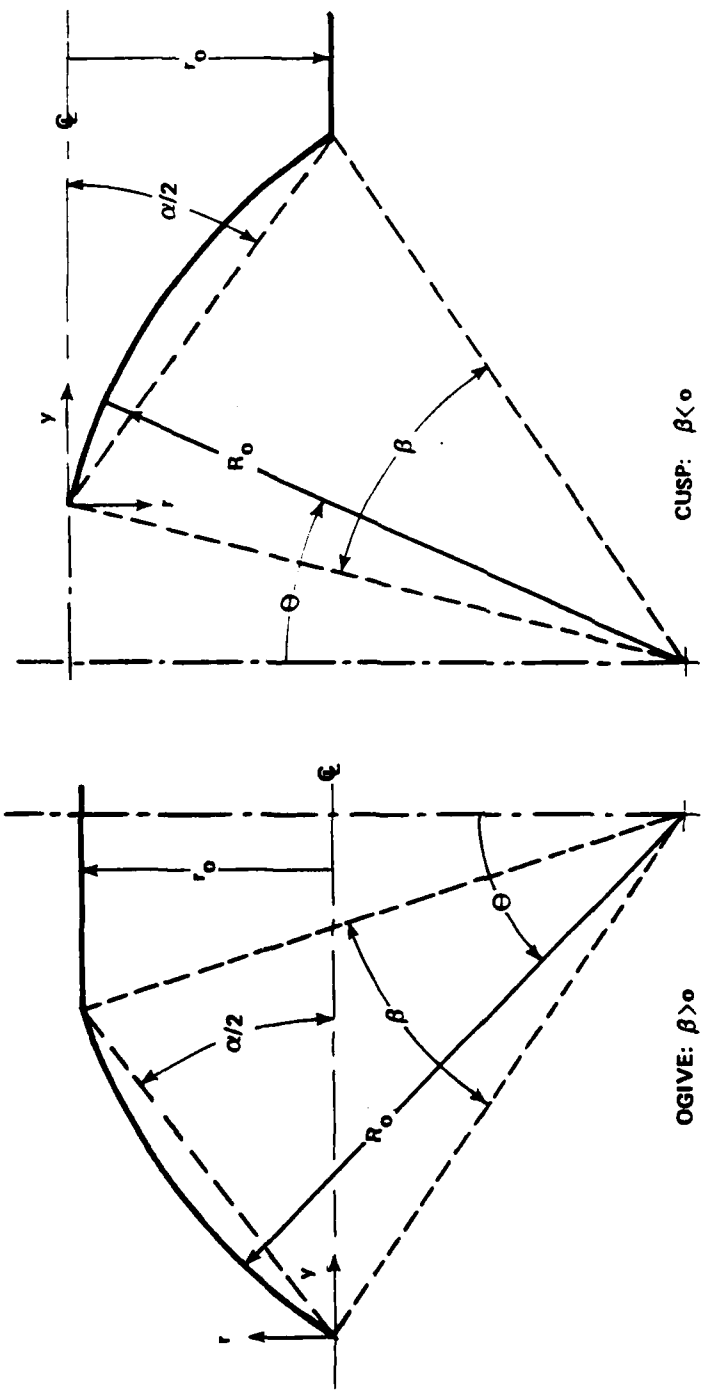

$R_o = r_o/2 \sin(\frac{\beta}{2}) \sin(\frac{\alpha}{2})$

$r = R_o[\cos\theta - \cos(\alpha + \beta)/2]$

$y = R_o[\sin(\alpha+\beta)/2 - \sin\theta]$

FIGURE 3 GEOMETRY OF OGIVES AND CUSPS

The test data for ogives and cusps, obtained from Reference 5, were correlated and tabulated in Tables 4 thru 7 for the 88.4/32, 60/43, 88.84/-31 and 59.94/-43.4 ogives. The correlations with $A_3 = 0$ and $A_3 = A_2$ appear to be comparable. For the ogives, both correlations are in good agreement with the test data and, excluding one data point, are well within the variation of the test data. The correlations for the cusps, although not always within the variation of the experimental data, appear to be reasonably good.

The empirical constants obtained from the least-square-fit of the impact drag force data are tabulated in Table 8. The empirical constants for $A_3 = 0$ are also plotted in Figure 4. Correlation of the empirical constants appears to be a possibility, however, test data for additional geometries must be obtained and correlated before this can reasonably be attempted.

CONCLUSIONS AND RECOMMENDATIONS

The successful correlation of the experimental data for the impact drag coefficients for cones, ogives, cusps and the sphere indicates the usefulness of the drag model for correlating the impact drag coefficients for a wide range of water-entry configurations. The data base for water-entry forces should be extended and correlated. Hopefully, this would lead to the successful correlation of the empirical constants. The usefullness of having a general correlation model for predicting the impact drag forces during water-entry is obvious. Impact drag forces, for which there is no test data, could then be predicted with reasonable confidence in the results. A method for predicting the drag force in the transition phase, from impact drag to cavity-running drag, should also be developed. A drag model for the cavity-running phase has previously been developed and reported in Reference 8.

---

[5] See footnote 5 on page 6

[8] Gaula, J. R. and Smith, C. W., "A Drag Model For Cavitating Axisymmetric Bodies", NOLTR 73-173, Sept 1, 1973.

TABLE 4

IMPACT DRAG COEFFICIENT FOR 88.4/32 OGIVE

Depth Of Penetration	Experimental Results, Ref. (5)			Correlation, Eq. (35)			
	Average	Variation, %		$A_1 = .273$ $A_2 = 2.22$ $A_3 = 0.$		$A_1 = 1.03$ $A_2 = A_3 = 1.91$	
H/r_o	$\bar{C}_d$	Lowest (-)	Highest (+)	C_d	$\frac{C_d - \bar{C}_d}{\bar{C}_d}$ %	C_d	$\frac{C_d - \bar{C}_d}{\bar{C}_d}$ %
.22	.316	17.7	13.0	.312	-1.3	.312	-1.3
.352	.511	11.8	12.2	.508	- .5	.508	- .6
.4847	.624	8.3	9.5	.630	+ .9	.630	+1.0
.6167	.673	3.9	8.0	.676	+ .4	.676	+ .5
.6607	.678	4.4	8.0	.677	- .2	.677	- .2
.7067	.674	5.8	8.4	.671	- .5	.671	- .5
.7933	.638	11.0	11.0	.644	+1.0	.642	+ .7

TABLE 5

IMPACT DRAG COEFFICIENT FOR 60/43 OGIVE

Depth Of Penetration	Experimental Results, Ref. (5)			Correlation, Eq. (35)			
	Average	Variation, %		$A_1 = .397$ $A_2 = 2.17$ $A_3 = 0.$		$A_1 = .998$ $A_2 = A_3 = 1.73$	
H/r_o	$\bar{C}_d$	Lowest (-)	Highest (+)	C_d	$\frac{C_d - \bar{C}_d}{\bar{C}_d}$ %	C_d	$\frac{C_d - \bar{C}_d}{C_d}$ %
.242	.143	14.4	28.4	.130	-9.3	.129	-9.8
.3873	.228	8.5	13.9	.221	-2.9	.221	-3.2
.5333	.277	5.1	7.6	.281	+1.6	.281	+1.6
.680	.299	3.3	4.7	.306	+2.2	.306	+2.4
.7267	.302	3.4	3.9	.307	+1.5	.307	+1.7
.7733	.300	3.1	3.5	.304	+1.5	.305	+1.6
.8733	.293	3.3	3.6	.291	- .6	.291	- .6
.9667	.279	2.8	3.6	.270	-3.1	.270	-3.3

TABLE 6

IMPACT DRAG COEFFICIENT FOR 88.34/-31 OGIVE

Depth Of Penetration	Experimental Results, Ref. (5)			Correlation, Eq. (35)			
	Average	Variation, %		$A_1 = 2.17$ $A_2 = 2.21$ $A_3 = 0.$		$A_1 = 3.11$ $A_2 = A_3 = 1.18$	
H/r_o	$\bar{C}_d$	Lowest (-)	Highest (+)	C_d	$\frac{C_d - \bar{C}_d}{\bar{C}_d}$ %	C_d	$\frac{C_d - \bar{C}_d}{\bar{C}_d}$ %
.28	.061	46.2	62.9	.061	- .8	.065	+ 6.4
.452	.201	14.0	12.4	.232	+15.6	.241	+20.1
.624	.617	4.6	11.1	.671	+ 8.7	.678	+ 9.9
.7933	1.83	4.7	6.2	1.73	- 5.3	1.73	- 5.6
.8533	2.38	4.2	2.9	2.43	+ 2.2	2.43	+ 2.2

TABLE 7

IMPACT DRAG COEFFICIENT FOR 59.94/-43.4 OGIVE

Depth Of Penetration	Experimental Results, Ref. (5)			Correlation, Eq. (35)			
	Average	Variation, %		$A_1 = 2.23$ $A_2 = 2.62$ $A_3 = 0.$		$A_1 = 2.80$ $A_2 = A_3 = 1.53$	
H/r_o	$\bar{C}_d$	Lowest (-)	Highest (+)	C_d	$\frac{C_d - \bar{C}_d}{\bar{C}_d}$ %	C_d	$\frac{C_d - \bar{C}_d}{\bar{C}_d}$ %
.598	.0206	75.8	268.5	.016	-22.2	.017	-15.5
.8934	.064	65.4	82.3	.082	+27.7	.086	+33.6
1.1867	.269	11.4	20.2	.306	+13.7	.310	+15.3
1.480	1.06	4.5	7.8	1.01	- 4.7	1.01	- 4.9
1.580	1.49	4.2	7.2	1.51	+ 1.7	1.52	+ 1.7

TABLE 8

SUMMARY OF EMPIRICAL CONSTANTS

Ogive	A_1			A_2		
α/β	$A_3 = 0$	$A_3 = A_2/2$	$A_3 = A_2$	$A_3 = 0$	$A_3 = A_2/2$	$A_3 = A_2$
59.94/-43.4	2.2334	2.5897	2.8006	2.6238	1.9346	1.5305
60/0	.447	.447	.447	2.1052	2.1052	2.1052
60/43	.3967	.7309	.9984	2.1656	1.9252	1.7328
88.84/-31	2.1726	2.7841	3.1134	2.2136	1.5389	1.1781
90/0	.447	.447	.447	2.1052	2.1052	2.1052
88.4/32	.2729	.6785	1.0282	2.2174	2.0536	1.9123
90/90	.6254	.9111	1.2619	.8820	.9724	1.0828

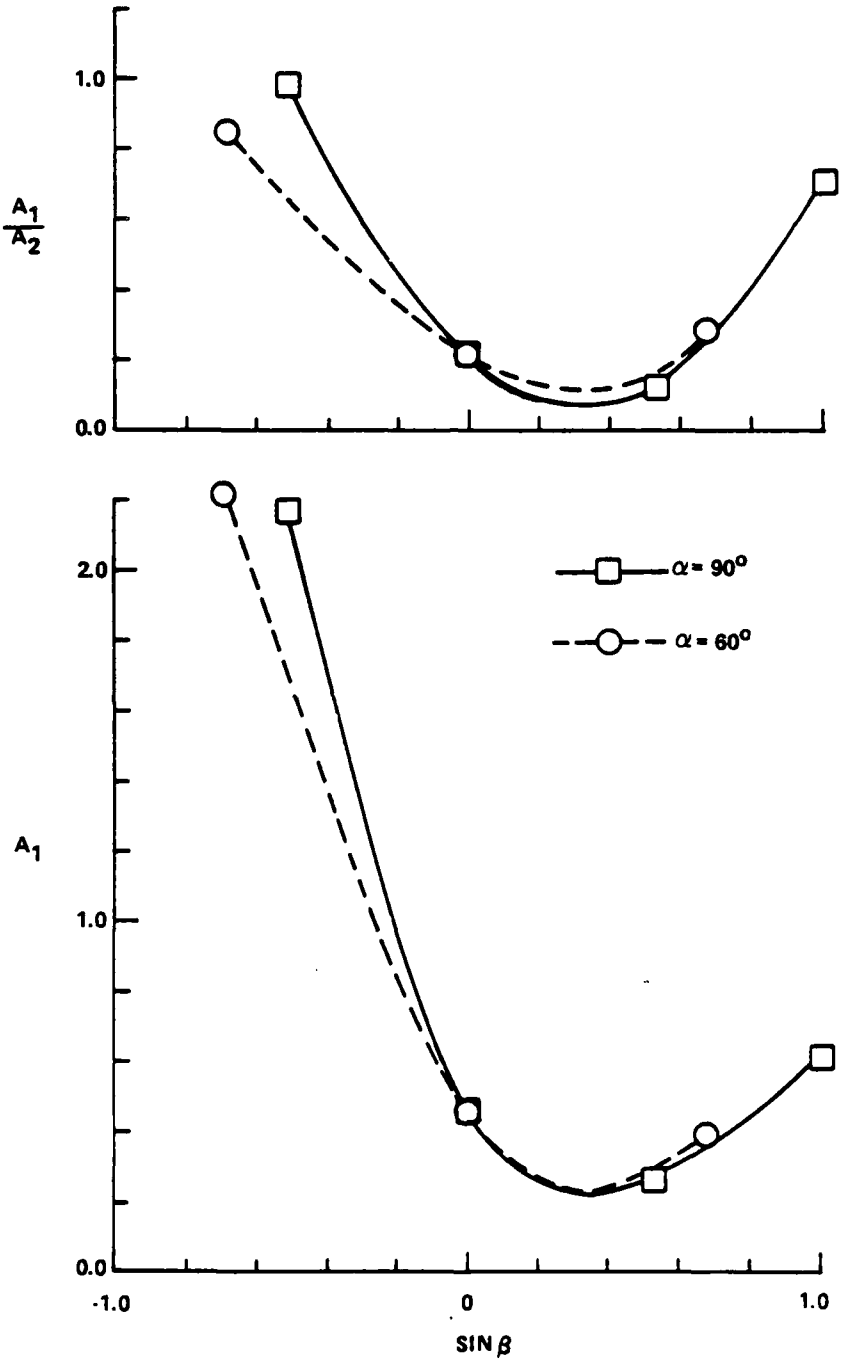

FIGURE 4 EMPIRICAL CONSTANTS (WITH $A_3 = o$) VS SIN β

APPENDIX A

POTENTIAL FLOW SOLUTION FOR THE AXIAL MOTION OF ELLIPSOIDS OF REVOLUTION

Semi-elliptic coordinates (μ, ζ, ω) are defined in Reference 9 in terms of the cylindrical coordinates (x, r, ω):

$$x = E\,\mu\,\zeta \tag{A-1}$$

$$r = E\,\xi\sqrt{1 - \mu^2} \tag{A-2}$$

$$\omega = \omega \tag{A-3}$$

Where E and ξ, defined in Table A-1, are introduced to alleviate the need to distinquish between ovary and planetary ellipsoids.

The surface of the moving ellipsoid, $\zeta = \zeta_o$, is defined:

$$\left(\frac{x}{a}\right)^2 + \left(\frac{r}{b}\right)^2 = 1 \tag{A-10}$$

Substituting for x and r from equations (A-1) and (A-2), the following values for ζ and ξ on the surface of the ellipsoid are obtained:

$$\zeta_o = \frac{a}{E} \tag{A-11}$$

$$\xi_o = \frac{b}{E} \tag{A-12}$$

The line elements in semi-elliptic coordinates have the value, Reference 9:

$$ds_\mu = \sqrt{\frac{E\nu}{1 - \mu^2}}\,d\mu \tag{A-13}$$

---

[9] Munk, M. M., "Ellipsoids Of Revolution", Chapter VII, Division C, Volume I, Of "Aerodynamic Theory", W. F. Durand, Dover Publications Inc., N. Y., 1963.

TABLE A-1

NOMENCLATURE FOR

OVARY AND PLANETARY ELLIPSOIDS

	Planetary, b>a	Ovary, a>b	
E^2	$+ (b^2 - a^2)$	$- (b^2 - a^2)$	(A-4)
ξ^2	$\zeta^2 + 1$	$\zeta^2 - 1$	(A-5)
ν^2	$\zeta^2 + \mu^2$	$\zeta^2 - \mu^2$	(A-6)
$f(\zeta)$	$\cot^{-1} \zeta$	$\frac{1}{2} \ln \frac{\zeta + 1}{\zeta - 1}$	(A-7)
$F(\zeta)$	$+\left[\frac{2}{\zeta} - 2 f(\zeta)\right]$	$-\left[\frac{2}{\zeta} - 2 f(\zeta)\right]$	(A-8)
$G(\gamma)$	$\frac{\cos^{-1} \gamma}{\sqrt{1 - \gamma^2}}$	$\frac{\ln\left[\gamma + \sqrt{\gamma^2 - 1}\right]}{\sqrt{\gamma^2 - 1}}$	(A-9)

$$ds_\zeta = \frac{E\nu}{\xi} \, d\zeta \tag{A-14}$$

$$ds_\omega = E \, \xi \sqrt{1 - \mu^2} \, d\omega \tag{A-15}$$

Where ν is defined in Table A-1. The velocity components, in terms of the velocity potential, ϕ, are:

$$V_\mu = - \frac{\partial \phi}{\partial S_\mu} = - \frac{\sqrt{1 - \mu^2}}{E\nu} \frac{\partial \phi}{\partial \mu} \tag{A-16}$$

$$V_\zeta = - \frac{\partial \phi}{\partial S_\zeta} = - \frac{\xi}{E\nu} \frac{\partial \phi}{\partial \zeta} \tag{A-17}$$

$$V_\omega = - \frac{\partial \phi}{\partial S_\omega} = - \frac{1}{E \, \xi \sqrt{1 - \mu^2}} \frac{\partial \phi}{\partial \omega} \tag{A-18}$$

The velocity potential for the axial motion of an ellipsoid in an infinite inviscid fluid is well known, Reference 9. The velocity potential can be expressed:

$$\phi = E \, K_1 \, \dot{A} \, \mu \, \zeta \, F(\zeta)/F(\zeta_o) \tag{A-19}$$

Where K_1 is the inertial factor for axial motion:

$$K_1 = \frac{\alpha_o}{2 - \alpha_o} \tag{A-20}$$

and:

$$\alpha_o = \zeta_o \, \xi_o^2 \, F(\zeta_o) \tag{A-21}$$

or, in terms of the fineness ratio, $\gamma = \frac{a}{b}$:

$$\alpha_o = \frac{2}{1 - \gamma^2} \left[\, 1 - \gamma \, G(\gamma) \, \right] \tag{A-22}$$

$F(\zeta)$ and $G(\gamma)$ are defined in Table A-1.

Substituting equation (A-19), for the velocity potential, into equations (A-16) thru (A-18), the velocity field is obtained:

$$V_\mu = - \frac{K_1 \, \dot{A}}{F(\zeta_o)} \frac{\sqrt{1 - \mu^2}}{\nu} \, \zeta \, F(\zeta) \tag{A-23}$$

[9] See footnote 9 on page 26

$$V_\zeta = - \frac{K_1 \dot{A}}{F(\zeta_o)} \quad \frac{\mu \xi}{\nu} \left[F(\zeta) - \frac{2}{\zeta \xi^2} \right] \tag{A-24}$$

$$V_\omega = 0 \tag{A-25}$$

It is assumed that the plane of the heaved free surface:

$$\eta (r, t) = - z \tag{A-26}$$

is in the equatorial plane of the moving ellipsoid:

$$\mu = o \tag{A-27}$$

In this plane the velocity of the fluid, and therefore the free surface, is vertically upward (see Figure 1):

$$\dot{\eta} = \frac{\partial \eta}{\partial t} = - V_{\mu \Big|_{\mu=o}} = K_1 \dot{A} F(\zeta)/F(\zeta_o) \tag{A-28}$$

On the intersection of the heaved free surface and the ellipsoid, $\zeta = \zeta_o$:

$$\dot{h} - \dot{H} = \dot{\eta}\Big|_{\zeta=\zeta_o} = K_1 \dot{A} \tag{A-29}$$

The mass flow rate at the heaved free surface can be expressed:

$$\dot{m} = 2\pi\rho \int_b^\infty \dot{\eta}\, r dr \tag{A-30}$$

An expression for rdr can be obtained from equation (A-2):

$$rdr = E^2 \left[(1 - \mu^2)\, \zeta d\zeta - \xi^2\, \mu d\mu \right] \tag{A-31}$$

On the surface, $\mu = o$, equation (A-31) becomes:

$$rdr = E^2\, \zeta d\zeta \tag{A-32}$$

Substituting equations (A-32) and (A-28) into equation (A-30):

$$\dot{m} = 2\pi\rho\, E^2 \frac{K_1 \dot{A}}{F(\zeta_o)} \int_{\zeta_o}^\infty F(\zeta)\, \zeta d\zeta \tag{A-33}$$

Since:

$$\int_{\zeta_o}^{\infty} F(\zeta)\, \zeta d\zeta = \frac{2 - \alpha_o}{2\, \zeta_o} \tag{A-34}$$

and from equations (A-21), (A-20) and (A-12) respectively :

$$F(\zeta_o) = \frac{\alpha_o}{\zeta_o\, \xi_o^2} \quad , \quad K_1 = \frac{\alpha_o}{2 - \alpha_o} \quad , \quad b^2 = E^2\, \xi_o^2$$

equation (A-33) becomes:

$$\dot{m} = 2\pi\rho \int_b^{\infty} \dot{\eta}\, r dr = \rho\pi b^2\, \dot{A} \tag{A-35}$$

Due to rotational symmetry, the total momentum of the fluid is directed vertically downward:

$$P = M\dot{H} = 2\pi\rho \iint U\, r dr\, dx = -\, 2\pi\rho \iint \frac{\partial\phi}{\partial x}\, r dr\, dx$$

$$= 2\pi\rho \int_{\mu=1}^{\mu=o} \phi\Big|_{\xi=\zeta_o} r dr + 2\pi\rho \int_{\zeta=\zeta_o}^{\zeta\to\infty} \phi\Big|_{\mu=o} r dr$$

$$- 2\pi\rho \int \phi\Big|_{x\to\infty} r dr \tag{A-36}$$

On the surface $x \to \infty$ and on the heaved free surface, $\mu = 0$, the velocity potential is zero ($\phi = 0$) and equation (A-36) becomes:

$$P = M\dot{H} = 2\pi\rho \int_{\mu=1}^{\mu=0} \phi\Big|_{\zeta=\zeta_o} r dr \tag{A-37}$$

On the surface of the ellipsoid, $\zeta = \zeta_o$, equations (A-19) and (A-31) become, respectively:

$$\phi\Big|_{\zeta=\zeta_o} = E\, \zeta_o\, K_1\, \dot{A}\, \mu = a\, K_1\, \dot{A}\, \mu \tag{A-38}$$

$$r dr = -\, E^2\, \xi_o^2\, \mu d\mu = -\, b^2\, \mu d\mu \tag{A-39}$$

Substituting into equation (A-37):

$$P = M\dot{H} = 2\pi\rho\, K_1\, \dot{A}\, ab^2 \int_0^1 \mu^2\, d\mu$$

$$= \frac{2}{3}\, \rho\pi b^2\, a\, K_1\, \dot{A} \qquad \text{(A-40)}$$

BIBLIOGRAPHY

Baldwin, J. L. and Steves, H. K., "Vertical Water-Entry of Spheres", NSWC/WOL/TR 75-49, May 1975.

Baldwin, J. L., "Vertical Water-Entry of Cones" NOLTR 71-25, February 1971.

Baldwin, J. L., "Vertical Water-Entry of Some Ogives, Cones, and Cusps", NSWC/WOL/TR 75-20, March 1975.

Gaula, J. R. and Smith, C. W., "A Drag Model For Caviting Axisymmetric Bodies", NOLTR 73-173, Sept 1, 1973.

May, A., "Water-Entry and the Cavity-Running Behavior of Missiles", SEA HAC/TR 75-2, 1975.

Munk, M. M., "Ellipsoids Of Revolution", Chapter VII, Division C, Volume I, Of "Aerodynamic Theory", W. F. Durand, Dover Publications Inc., N. Y., 1963.

Shiffman, M. and Spencer, D. C., "Force of Impact On a Cone Striking a Water Surface (Vertical Entry)", Comm. Pure and Appl. Math., Vol IV (1951).

Smith, C. W., "Experimental Investigation of the Behavior of Vertical Water-Entry Cavities", NSWC/WOL/TR 78-135, September 1978.

Wardlaw, A. B., Morrison, A. M. and Baldwin, J. L., "Prediction Of Impact Pressure Pressures, Forces, and Moments During Vertical and Oblique Water-Entry", NSWC/WOL/TR 77-16, January 1977.

DISTRIBUTION

	Copies
Commander Naval Sea Systems Command Department of the Navy ATTN: SEA-09G32 SEA-03B SEA-880, T. Pierce Washington, DC 20362	 2 1 1
Office of Naval Research 800 N. Quincy St. ATTN: Code 438 Arlington, VA 22217	 2
Library of Congress ATTN: Gift and Exchange Division Washington, DC 20540	 4
Defense Technical Information Center Cameron Station ATTN: Distribution Statement A Alexandria, VA 22314	 12
Director Defense Research and Engineering The Pentagon Washington, DC 20301	
Director of Research National Aeronautics and Space Administration 600 Independence Avenue Southwest Washington, DC 20546	
NASA Scientific and Technical Information Facility Post Office Box 33 College Park, MD 20740	
Director Alden Research Laboratories Worcester Polytechnic Institute Holden, MA 01520	

Copies

Applied Physics Laboratory
The Johns Hopkins University
Johns Hopkins Road
ATTN: Document Librarian
Laurel, MD 20810

Applied Research Laboratory
The Pennsylvania State University
Post Office Box 30
ATTN: Library
Dr. J. W. Holl
State College, PA 16801

Superintendent
U. S. Naval Postgraduate School
ATTN: Library
Monterey, CA 93940

Commanding Officer
U. S. Naval Air Development Center
ATTN: NADC Library
Warminister, PA 18974

Director
U. S. Naval Research Laboratory
ATTN: Library
Washington, DC 20390

Commanding Officer
David Taylor Naval Ship Research and Development Center
ATTN: Library
Bethesda, MD 20084

Commander
Naval Ocean Systems Center
San Diego, CA 92132

Commanding Officer
Naval Underwater Systems Center
Newport, RI 02840

Commander
Naval Weapons Center
ATTN: Library
China Lake, CA 93555

Harry Diamond Laboratories
2800 Powder Mill Rd., Adelphi, Maryland 20783

Hydronautics, Incorporated
Pindell School Road
Laurel, MD 20810

Copies

Iowa Institute of Hydraulic Research
State University of Iowa
Iowa City, Iowa 52240

California Institute of Technology
Pasadena, CA 91109

Massachusetts Institute of Technology
Cambridge, MA 02139

NDW-NSWC(W)-5605/1 (Rev. 5-78)

TO AID IN UPDATING THE DISTRIBUTION LIST FOR NAVAL SURFACE WEAPONS CENTER, WHITE OAK TECHNICAL REPORTS PLEASE COMPLETE THE FORM BELOW:

TO ALL HOLDERS OF NSWC TR 80-243
by Charles Smith, U23

DO NOT RETURN THIS FORM IF ALL INFORMATION IS CURRENT

A. FACILITY NAME AND ADDRESS *(OLD) (Show Zip Code)*

NEW ADDRESS *(Show Zip Code)*

B. ATTENTION LINE ADDRESSES:

C.

☐ REMOVE THIS FACILITY FROM THE DISTRIBUTION LIST FOR TECHNICAL REPORTS ON THIS SUBJECT.

D.

NUMBER OF COPIES DESIRED _____

GPO 930-784

DEPARTMENT OF THE NAVY
NAVAL SURFACE WEAPONS CENTER
WHITE OAK, SILVER SPRING, MD. 20910

OFFICIAL BUSINESS
PENALTY FOR PRIVATE USE, $300

POSTAGE AND FEES PAID
DEPARTMENT OF THE NAVY
DOD 316

COMMANDER
NAVAL SURFACE WEAPONS CENTER
WHITE OAK, SILVER SPRING, MARYLAND 20910

ATTENTION: CODE U23


DATE:
ILME